ORIGINAL PAPER

THE INFLUENCE OF THE SOLAR THERMAL COLLECTORS INTEGRATED INTO THE BUILDING FAÇADE ON THE BUILDING THERMAL ENERGY DEMAND ACROSS EUROPE

MACEDON MOLDOVAN[1], ION VISA[1], IOANA DENISA RUSEA[1]

Manuscript received: 15.12.2029; Accepted paper: 04.02.2020;

Published online: 30.03.2020.

Abstract. *The influence of the building-integrated solar thermal collectors on the thermal energy demand of a laboratory building considering eight sites across Europe is analyzed. TRNSYS was used to evaluate the thermal energy demand for buildings with standard (40 mm) and increased (60 mm to 210 mm) thickness of the insulated panels aiming to reach a specific thermal energy demand lower than 100 kWh/m²/year. For each building optimized in terms of thermal insulation, a sensitivity analysis was performed to assess the influence of the collectors' air gap and glazing thickness, absorber plate color, resulting in heating energy reductions up to 23.59%.*

Keywords: *solar thermal façade, building thermal energy demand, low energy building, nearly zero energy building.*

1. INTRODUCTION

The Nearly Zero Energy Building standard introduced by 2010/31/EU Directive is mandatory since 1st January 2019 for new public buildings in Europe and will enter in force by 31st December 2020 for all new buildings [1]. The Directive imposes energy efficiency measures to significantly decrease the building's energy demand and to cover it with renewable energy, at cost-optimal levels. Solutions to decrease the thermal transfer through the building facades range nowadays from traditional thermal insulation materials (e.g. polystyrene, mineral wool etc.) to phase change materials [2], nano vacuum insulation panels [3], aerogel [4] and even more advanced solutions as the biomimetic facades [5].

Thermal energy represents the largest share in the buildings' energy demand. Solar thermal collectors are usually implemented on the buildings' roofs to prepare domestic hot water. These solar thermal collectors can partly cover the thermal energy demand for space heating but their number must be increased requiring a larger roof surface. Buildings' facades are good candidates to install solar thermal collectors. By integrating the solar thermal collectors in the building facades (preferably at the same time with their thermal insulation), building integrated solar thermal collectors (BISTC) are obtained. Thus, both targets of the 2010/31/EU Directive are addressed: increased energy efficiency and a larger share of energy demand covered form renewable energy sources. During the past two decades, intensive research was developed on both opaque and transparent solar facades. For opaque BISTC, one of the first applied solutions, demonstrating good potential in reducing the building heating load [6], was the thermal storage wall or Trombe wall, consisting of a massive, not insulated,

[1] Transilvania University of Brasov, Renewable Energy Systems and Recycling Research Centre, 500036 Brasov, Romania. E-mail: macedon.moldovan@unitbv.ro, visaion@unitbv.ro, ioana.rusea@unitbv.ro.

south oriented wall fitted with glazing. The produced thermal energy is transferred to the building through natural or forced ventilation of the air heated in front of the wall or through the forced circulation of water within copper pipes embedded in the concrete wall [7]. To further increase the efficiency of the solar to thermal energy conversion, spectral selective absorber plates and thermal insulation are embedded in the building facades, transferring the thermal energy to the building through a thermal fluid (air or water) [8]. To improve the architectural and social acceptance, novel façade integrated solar thermal collectors with various design solutions were proposed to be integrated into the building's facade [9]. Novel flat plate solar thermal collectors with trapezoidal [10] and triangle [11] shape and various colors were designed and experimentally optimized [12].

Besides the thermal energy output useful for domestic hot water preparation and for space heating, the BISTC concept offers several additional advantages: a) the cost of collectors is decreased because the thermal insulation and the back plate are no longer required, as the building's thermal insulation is also used for the solar collector; b) the BISTC surface and that of the interconnection pipes exposed to the open environment is lowered at maximum, thus the thermal losses are decreased resulting in an increased conversion efficiency; c) the cost of the piping system is lowered as shorter pipes are required to connect the BISTC with the storage tanks, that can be distributed in the technical rooms at the same floor with the façade accommodating the BISTC; d) the thermal effect obtained in the BISTC is beneficial for the building's insulation, e.g. during the cold season, in the winter days with low solar irradiance; e) during the summer days, the building's envelope is not directly heated by the solar radiation which will be blocked (and used) by the BISTC, thus the heating effect on the building is decreased or eliminated when a larger thermal fluid flow is employed; this can be further used, e.g. for a heating a swimming pool; f) the colour of the façade can be obtained by variously coloured BISTC absorber plate, better protected by glazing, thus decreasing the overall costs of the façade finishing materials and maintenance, and increasing the architectural acceptance; g) increase coverage degree of the façade with solar thermal collectors by using non-conventional collector shapes (e.g. trapezoidal, triangular etc.); h) improving sound protection [13-15].

The paper focuses on the passive influence of the BISTC on the thermal energy demand for space heating and cooling. Trnsys was used to simulate the thermal energy demand of a building with and without BISTC. The study was further developed to outline which parameter (thermal insulation -, air gap -, glazing thickness, and absorber plate colour) is most influential when considering buildings implemented at eight sites across Europe. Recommendations of novel BISTC designs with high architectural acceptance are proposed for new buildings and for the existing building stock, which represents more than 90% in Europe.

2. METHODS

The following algorithm is proposed to evaluate the influence of the BISTC on the building thermal energy demand for space heating and cooling:

Step 1. Assessing the thermal energy demand for the reference case. As the reference case, the building is considered without BISTC, having white facades and constant thickness of thermal insulation.

Step 2. Estimating the influence of the thermal insulation. The thickness of the thermal insulation is modified in order to get similar specific thermal energy demand (kWh/m²/year under an imposed limit) in each implementation site, chosen for the building.

Step 3. Estimating the influence of the air gap thickness. For each optimally insulated building, a 5 mm thick glazing is considered, mounted in front of the white Southern façade at variable distances (air gap thickness) between 5 mm to 30 mm.

Step 4. Estimating the influence of the absorber plate color. For the optimal air gap thickness obtained in Step 3, a colored absorber plate (black, blue, green, orange, red and sandstone) is considered to be mounted between the air layer and the thermal insulation of the Southern façade.

Step 5. Estimating the influence of the glazing thickness. For the black absorber, the influence of glazing thickness is tested considering values from 3 mm to 10 mm.

3. CASE STUDY

A small (30 m²) laboratory building was considered as a case study (Fig.1). It is a modular construction implemented in the Renewable Energy Systems and Recycling (RESREC) R&D Centre in the Transilvania University of Brasov, Romania, as an outdoor testing rig for solar thermal collectors. The building consists of a metallic frame and 40 mm thick insulating panels as exterior walls and horizontal rooftop. This assembly is installed on a ground level concrete slab. Extruded polystyrene insulation with a thickness of 40 mm is used between the concrete slab and the ground. The main geometrical features of the building are presented in Table 1.

Figure 1. The outdoor testing rig for solar thermal collectors considered in the study.

Table 1. Geometrical characteristics of the laboratory building.

Characteristic	M.U.	Value
Length/Width/Height	m	6 / 5 / 2.5
Total floor surface	m²	30
Exterior walls surface (including windows)	m²	55
Windows and door surface	m²	5
Envelope surface	m²	115
Volume	m³	75
Window to wall ratio	m² / m²	0.09
Building shape factor	m² / m³	1.53

This laboratory was modelled as a 3D building using Trnsys3d for SketchUp with a single zone (Fig. 2). The building has one exterior door on the Eastern façade, two windows

on the Northern façade and another window on the Western façade. The Southern façade was left free of windows; to maximize the available area for façade integrated solar thermal collectors.

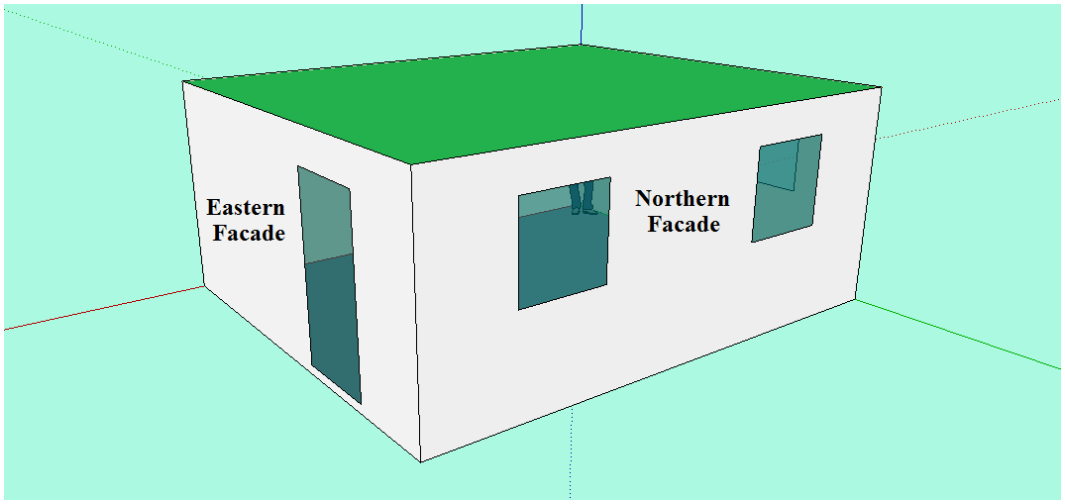

Figure 2. Three dimensional building modelled in Trnsys3d.

The model was imported in TRNBuild where eight European implementation sites were considered. These locations are presented in Table 2, considering the latitudes, along with the main meteorological characteristics obtained from the Meteonorm software; for Brasov the data were on site measured with a Solys2 sun tracker from Kipp&Zonen (direct solar irradiance, horizontal global irradiance and horizontal diffuse solar irradiance) and a DeltaT weather station (outdoor air temperature and relative humidity, wind speed and direction, precipitation level). For each location, the building was considered with the same orientation. The locations were chosen spread all over the latitudes in Europe, to estimate the influence of the location on the thermal energy demand (for space heating, space cooling and DHW) of a building with and without BISTC incorporated in the Southern façade.

Table 2. Considered implementation sistes for the case study building.

Location	Latitude	Longitude	Climate	Global solar energy EGh [kWh/m²]	Mean temperature of the outdoor air ta [°C]	Mean temperature of the cold water tw [°C]
Finland, Helsinki	60.19	24.95	humid continental	947	4.52	7.86
Germany, Hamburg	53.55	9.99	oceanic climate	952	8.85	12.19
Ireland, Dublin	53.35	-6.27	maritime climate	948	9.48	12.82
Netherlands, Amsterdam	52.37	4.90	oceanic climate	987	9.51	12.85
Austria, Graz	47.08	15.42	humid continental	1143	8.41	11.74
Romania, Brasov	45.65	25.61	temperate continental	1293	9.90	13.24
Portugal, Lisbon	38.74	-9.14	subtropical climate	1683	16.81	20.14
Cyprus, Larnaca	34.87	33.61	semi-arid climate	1847	18.98	22.31

The laboratory is an office building with specific regime data presented in Table 3. The building is occupied only during working days, between 08:00 and 17:00. Ventilation was not considered as the infiltration air change rate is covering the fresh air demand.

Table 3. Regime data for the case study building.

Regime	M.U.	Value
Infiltration airchange rate	h^{-1}	0.5
Heating		
- set point temperature	°C	20
- power	kJ / h	unlimited
- humidification	%	off
Cooling		
- set point temperature	°C	24
- power	kJ / h	unlimited
- humidification	%	off
Gains		
- number of occupants	persons	2
- degree of activity		seated, light work
- rate of heat gain from occupants	W	150
- rate of heat gain from appliances	W	230
- rate of heat gain from artificial lighting	W / m²	5
- convective part of artificial lighting	%	10
- turn light ON if horizontal irradiance is lower than	W / m²	120
- turn light OFF if horizontal irradiance is higher than	W / m²	200
Initial values		
- initial zone temperature	°C	20
- initial relative humidity	%	50

Based on the regime data presented in Table 3, numerical simulations were performed in Trnsys17 Simulation Studio, where a new MultiZone Building project was developed with the structure presented in Fig. 3. The TRNBuild building file was imported as a Type56 unit, onsite measured meteorological data were imported into the Type 15-2 Weather data unit, and equation cards were used to calculate the azimuth angles of the building's envelope components and associated solar irradiances.

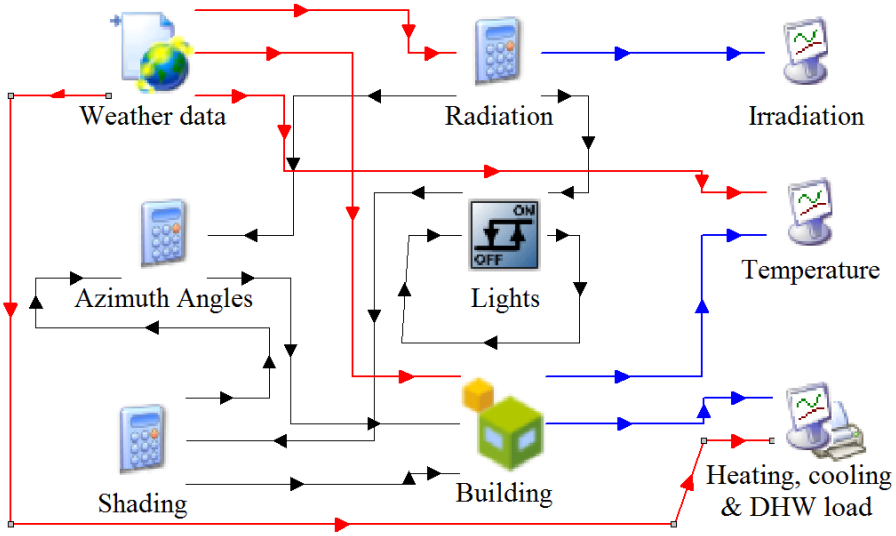

Figure 3. The outdoor testing rig for solar thermal collectors considered in the study.

The daily energy demand for domestic hot water is numerically simulated over one year considering a number of two persons for each site. Output data (irradiance on each building's envelope component, outdoor air temperature, water mean temperature, indoor air temperature, heating and cooling load) were plotted and exported in csv files through Type 65a online plotter units. Output data are presented and discussed in the next section.

4. RESULTS AND DISCUSSION

The algorithm presented in the second section was applied for each selected location as follows.

Step1. The yearly thermal energy demand is obtained through TRNSYS numerical simulations for the eight locations considered as case study buildings, without BISTC on the Southern façade. The hourly variation of the components in thermal the energy demand are presented in Fig. 4 along with the outdoor air and cold water temperatures for Brasov, Romania. The outdoor air temperature ranges between -20°C and 33.4°C and the cold water temperature varies between 8.11°C and 18.37°C. According to these input parameters along with the solar irradiance and the regime imposed for the case study building, the heating/cooling power present values as high as 1946 W and 1021 W respectively. The results obtained for the eight locations are comparatively presented in the Table 4 showing a normal distribution, with higher heating energy demand for the Nordic latitudes and higher cooling energy demand for lower latitudes. The DHW energy demand is almost constant, and lower values are obtained in southern location due to the higher temperature of the cold water.

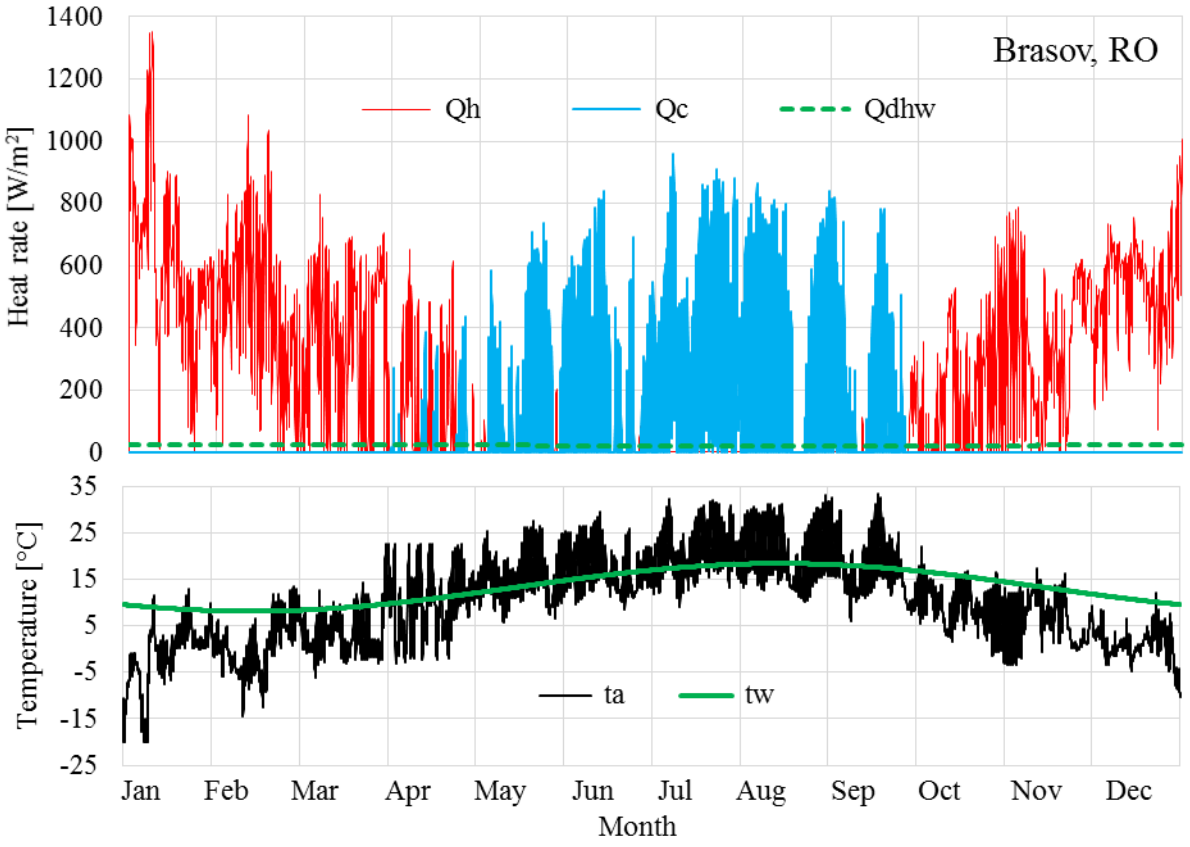

Figure 4. Hourly variation of the outdoor air temperature (ta), cold water temperature (tw) and of the thermal energy demand components for: space heating (Qh), space cooling (Qc) and DHW (Qdhw) for Brasov, Romania.

Table 4. Thermal energy demand of the buildings without BISTC in the southern facade.

Location	Thermal insulation thickness [mm]	Heating energy demand [kWh/year]	Cooling energy demand [kWh/year]	DHW energy demand [kWh/year]	Thermal energy demand [kWh/year]	Specific thermal energy demand [kWh/m²/year]
Finland, Helsinki	40	6010	97	221	6329	210.97
Germany, Hamburg	40	4160	100	202	4464	148.82
Ireland, Dublin	40	3626	9	200	3836	127.89
Netherlands Amsterdam	40	3709	69	200	3979	132.64
Austria, Graz	40	4283	180	204	4668	155.63
Romania, Brasov	40	3493	492	198	4184	139.47
Portugal, Lisbon	40	965	783	169	1917	63.93
Cyprus, Larnaca	40	728	1462	159	2351	78.37

Step 2. Further on, the optimal thickness of the thermal insulation was evaluated to obtain similar specific thermal energy demand values at each implementation location of the building (below 100 kWh/m²/year). The influence of the thermal insulation thickness on the thermal energy demand components is comparatively presented in Table 5 for the selected locations.

Table 5. Thermal energy demand of the buildings without BISTC in the southern facade.

Location	Thermal insulation thickness [mm]	Heating energy demand [kWh/year]	Cooling energy demand [kWh/year]	DHW energy demand [kWh/year]	Thermal energy demand [kWh/year]	Specific thermal energy demand [kWh/m²/year]
Finland, Helsinki	210	2099	657	221	2977	99.26
Germany, Hamburg	80	2486	241	202	2931	97.70
Ireland, Dublin	60	2644	18	200	2862	95.42
Netherlands Amsterdam	70	2391	147	200	2738	91.28
Austria, Graz	100	2183	463	204	2851	95.04
Romania, Brasov	90	1908	820	198	2927	97.57
Portugal, Lisbon	40	965	783	169	1917	63.93
Cyprus, Larnaca	40	728	1462	159	2351	78.37

Step 3. For each optimally insulated building presented in Table 5, a glazing with a 5 mm thickness was considered in the front of the white Southern façade. The variation of the

thermal energy demand for the various air gap thicknesses is presented in Fig. 5 for three locations, showing an optimal air gap thickness of 15 mm in all cases as there is no further significant decrease when considering higher values in the air gap. The optimal air gap thickness was evaluated for each location, and the results are comparatively presented in Table 6. The 15 mm was found as the optimal air gap for all the selected locations with similar influences on the components (space heating and space cooling) of the thermal energy demand.

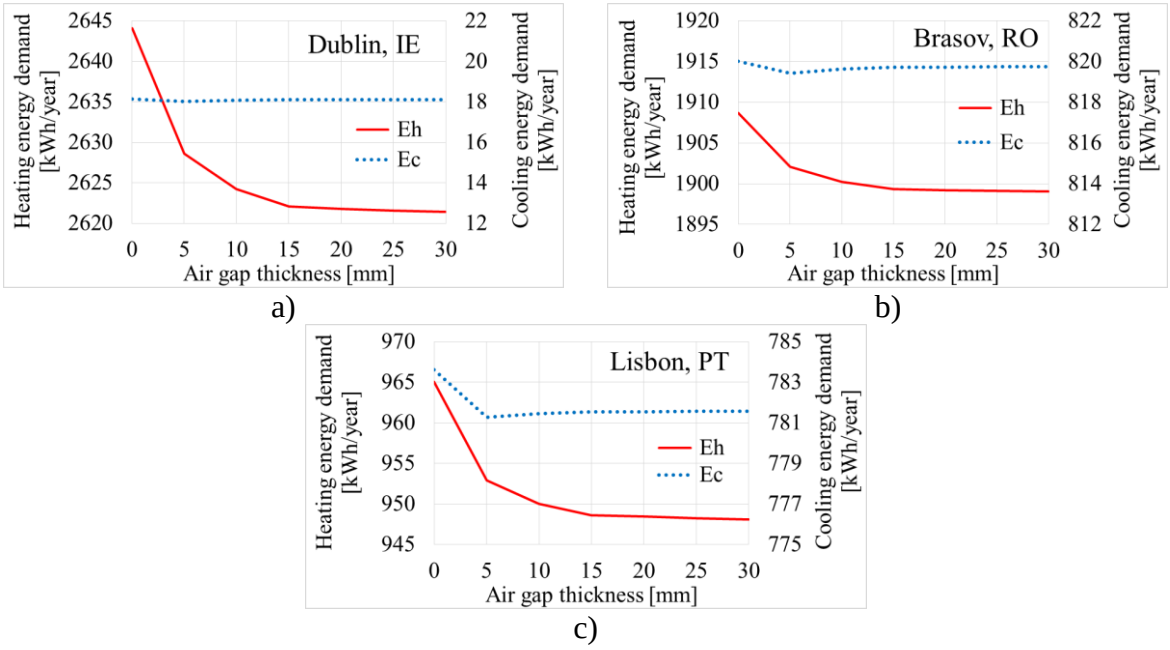

Figure 5. Effect of the air gap thickness on the thermal energy demand for space heating (Eh) and for cooling (Ec) the building for a) Dublin, IE, b) Brasov, RO and c) Lisbon, PT.

Table 6. Thermal energy demand of the buildings with glazing on the southern facade.

Location	Optimal air gap thickness [mm]	Heating energy demand [kWh/year]	Cooling energy demand [kWh/year]	DHW energy demand [kWh/year]	Thermal energy demand [kWh/year]	Specific thermal energy demand [kWh/m²/year]
Finland, Helsinki	15	2096	657	221	2975	99.19
Germany, Hamburg	15	2472	241	202	2916	97.22
Ireland, Dublin	15	2622	18	200	2840	94.68
Netherlands Amsterdam	15	2375	147	200	2722	90.75
Austria, Graz	15	2173	463	204	2841	94.72
Romania, Brasov	15	1899	819	198	2917	97.25
Portugal, Lisbon	15	948	781	169	1899	63.31
Cyprus, Larnaca	15	714	1456	159	2330	77.70

Step 4. Further on, for the optimal air gap thickness previously obtained, a coloured absorber plate (black, blue, green, orange, red and sandstone) is considered between the air

layer and the thermal insulation of the Southern façade. The influence of the absorber plate color on the heating and cooling energy demand is plotted in Fig. 6 for the buildings implemented in Dublin, Brasov and Lisbon. As expected, the black color has the largest influence on reducing the heating energy demand but also on the cooling energy demand, which increases if no heat removal is considered from the absorber plate. The results are comparatively presented for the selected locations in Table 7.

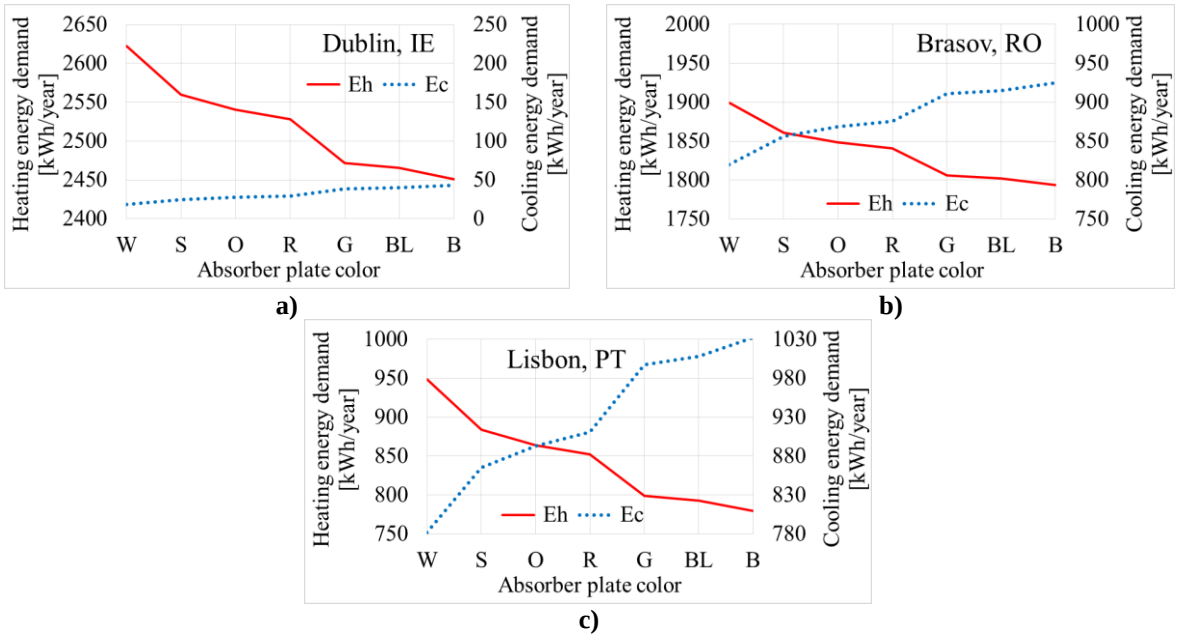

Figure 6. The heating/cooling energy demand for colored absorber plates (W – white, S – sandstone, O – orange, R – red, G – green, BL – blue and B – black) for: a), Dublin, IE, b) Brasov, RO and c) Lisbon, PT.

Table 7. Heating energy demand of the buildings with coloured BISTC on the southern facade.

Location	Color and absorptance factor [16] of the BISTC absorber plate						
	White	Sandstone	Orange	Red	Green	Blue	Black
	α = 0.26	α = 0.50	α = 0.58	α = 0.63	α = 0.88	α = 0.91	α = 0.98
	Heating energy demand [kWh/year]						
Finland, Helsinki	2096	2082	2077	2074	2061	2060	2056
Germany, Hamburg	2472	2435	242	2416	2382	2378	2369
Ireland, Dublin	2622	2559	2540	2528	2471	2465	2450
Netherlands, Amsterdam	2375	2327	231	2304	2261	2256	2245
Austria, Graz	2173	2136	2124	2117	2084	2080	2071
Romania, Brasov	1899	1860	1848	1841	1806	1802	1793
Portugal, Lisbon	948	883	864	852	798	792	779
Cyprus, Larnaca	714	652	634	623	574	569	557

Step 5. Further on, for the black absorber plate, the influence of the glazing thickness ranging from 3 mm to 10 mm was assessed. The results presented in Table 8 show that when increasing the glazing thickness, there only is a slight decrease in the heating energy demand. The glazing transmittance decreases with its thickness, reducing thus the solar energy received by the absorber and the thermal energy output [17]. Thus, the use of the lowest

possible thickness imposed by the mechanical resistance conditions is recommended. The mechanical resistance is directly influenced by the size of the BISTC and small-sized collectors (e.g. small triangle or trapeze collectors) allow the use of thinner glazing.

Table 8. Heating energy demand of the buildings with different glazing thickness of the black BISTC.

Location	Thickness of the BISTC glazing [mm]							
	3	4	5	6	7	8	9	10
	Heating energy demand [kWh/year]							
Finland, Helsinki	2057	2057	2056	2056	2055	2055	2054	2054
Germany, Hamburg	2370	2369	2369	2368	2368.	2367	2366	2366
Ireland, Dublin	2452	2451	2450	2449	2448	2447	2446	2444
Netherlands Amsterdam	2247	2246	2245	2244	2243	2242	2241	2240
Austria, Graz	2072	2072	2071	2070	2070	2069	2069	2068
Romania, Brasov	1794	1793	1793	1792	1792	1791	1791	1790
Portugal, Lisbon	783	781	779	777	775	773	771	769
Cyprus, Larnaca	561	559	557	554	552	550	547	545

Finally, the relative reduction in the heating energy demand is calculated for the building with BISTC mounted on the entire Southern façade, for a 5 mm glazing with an air gap of 15 mm and various colors of the absorber plate. The other parameters required for computing the heating energy demand are those presented in Section 3. The reference building in each location was considered the building with an insulation thickness designed to lower the specific thermal energy demand down to 100kWh/m². The results comparatively presented in Table 9, show relative reductions ranging between 0.14% and 23.59%. The lowest values correspond to the Nordic countries and light colors of the absorber plates.

Table 9. Heating energy demand relative reduction of the buildings with BISTC on the Southern facade.

Location	Color of the BISTC absorber plate						
	White	Sandstone	Orange	Red	Green	Blue	Black
	Relative reduction of the heating energy demand [%]						
Finland, Helsinki	0.14	0.82	1.04	1.17	1.79	1.87	2.03
Germany, Hamburg	0.57	2.07	2.54	2.83	4.20	4.36	4.72
Ireland, Dublin	0.83	3.19	3.93	4.38	6.52	6.76	7.31
Netherlands, Amsterdam	0.66	2.64	3.26	3.63	5.42	5.63	6.09
Austria, Graz	0.44	2.13	2.66	2.98	4.52	4.70	5.11
Romania, Brasov	0.49	2.53	3.16	3.54	5.37	5.57	6.05
Portugal, Lisbon	1.70	8.42	10.44	11.66	17.21	17.83	19.22
Cyprus, Larnaca	2.02	10.46	12.95	14.45	21.19	21.93	23.59

When the complete effect of the facades upgrading is considered (including the thermal insulation), the relative reduction in the heating energy demand is significantly higher in Nordic countries (Table 10).

Table 10. Heating energy demand relative reduction of the buildings after facades upgrading.

Location	Color of the BISTC absorber plate						
	White	Sandstone	Orange	Red	Green	Blue	Black
	Relative reduction of the heating energy demand [%]						
Finland, Helsinki	65.12	65.36	65.43	65.48	65.70	65.72	65.78
Germany, Hamburg	40.58	41.47	41.75	41.93	42.75	42.84	43.06
Ireland, Dublin	27.71	29.43	29.97	30.30	31.85	32.03	32.43
Netherlands, Amsterdam	35.97	37.25	37.65	37.89	39.04	39.17	39.47
Austria, Graz	49.26	50.12	50.39	50.56	51.34	51.43	51.64
Romania, Brasov	45.63	46.74	47.09	47.30	48.29	48.41	48.67
Portugal, Lisbon	1.70	8.42	10.44	11.66	17.21	17.83	19.22
Cyprus, Larnaca	2.02	10.46	12.95	14.45	21.19	21.93	23.59

All these estimations were developed considering BISTC mounted on the entire Southern façade of the building. To increase the architectural acceptance of these upgraded facades, non-rectangular shapes are proposed along with the various colors to fully or partly cover the Southern façade (Fig. 7). Thus, the architects have the possibility to combine different shapes and colors of the solar thermal collectors with the elements of the facades (windows, doors, etc.) to increase the architectural acceptance of the facade integrated solar thermal collectors.

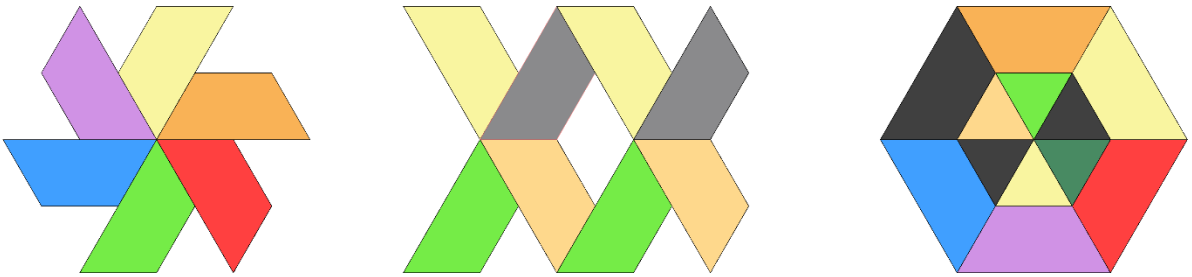

Figure 7. Proposed arrangements of trapezoidal solar thermal collectors variously coloured.

5. CONCLUSIONS

The effect of the building integrated solar thermal collectors (BISTC) on the Southern façade of a small outdoor laboratory is estimated in the paper considering eight European implementation locations. The thermal energy demand (for space heating, space cooling and DHW) of the building in its standard specification (metallic structure with 40 mm insulated panels) was calculated resulting specific thermal energy indicators between 63.93 kWh/m²/year for Lisbon and 210.97 kWh/m²/year for Helsinki. When the thermal insulation thickness was increased for the buildings consuming more than 63.93 kWh/m²/year, new values are obtained, ranging between 60 mm and 210 mm, depending on the climate type in the implementation location. For each improved building envelope, the influence of the BISTC on the entire southern façade was further assessed, resulting that heating energy reductions up to 23.59% can be obtained depending on the site location and on the color of the absorber plate color (at an optimal thickness of 15 mm for the air gap and 5 mm for the glazing). This demonstrates that the integration of BISTC in the

building façade is beneficial through the reduction of the heating energy demand of the building, besides the active role of BISTC – the conversion of the solar energy in thermal energy for DHW and also contributing to the space heating (at least in transition months). Further studies will be carried out to assess the influence of integrating the solar collector in the building façade, on the efficiency of the solar thermal collector/system. The outdoor laboratory will also be developed to experimentally investigate the mutual influence between BISTC and the building.

REFERENCES

[1] European Parliament, *Official Journal of the European Union*, **53**, 1, 2010.
[2] Fateh, A., Klinker, F., Brutting, M., Weinlader, H., *Energy and Buildings*, **153**, 231, 2017.
[3] Mujeebu, M. A., Ashraf N., Alsuwayigh, A. H., *Applied Energy*, **173**, 141, 2016.
[4] Jia, G., Li, Z., Liu, P., Jing, Q., *Journal of Non-Crystalline Solids*, **482**, 192, 2018.
[5] Webb, M., Aye, L., Green, R., *Applied Energy*, **213**, 670, 2018.
[6] Hu, Z., He, W., Ji, J., Zhang, S., *Renewable and Sustainable Energy Reviews*, **70**, 976, 2017.
[7] O'Hegarty, R., Kinnane, O., McCormack, S. J., *Applied Energy*, **206**, 1040, 2017.
[8] Zhang, X., Shen, J., Lu, Y., He, W., Xu, P., Zhao, X., Qiu, Z., Zhu, Z., Zhou, J., Dong, X., *Renewable and Sustainable Energy Reviews*, **50**, 32, 2015.
[9] Visa, I., Moldovan, M., Comsit, M., Neagoe, M., Duta, A., *Energy Procedia*, **112**, 176, 2017.
[10] Visa, I., Duta, A., Comsit, M., Moldovan, M., Ciobanu, D., Saulescu, R., Burduhos, B., *Applied Thermal Engineering*, **90**, 432, 2015.
[11] Visa, I., Moldovan, M., Duta, A., *Renewable Energy*, **143**, 252, 2019.
[12] Moldovan, M., Visa, I., *E3S Web of Conferences*, **85**, 04005, 2018.
[13] Vasile, I., Vasile, V., Miron-Alexe, V., Diaconu, E., Caciula, I., Andrei H., *Journal of Science and Arts*, **4**(41), 861, 2017.
[14] Vasile, I., Vasile, V., Diaconu, E., Andrei H., Angelescu, N., *Journal of Science and Arts*, **3**(48), 793, 2019.
[15] Miron-Alexe, V., Vasile, I., *Journal of Science and Arts*, **4**(41), 853, 2017.
[16] Owen, M.S. (Ed.), *ASHRAE Handbook—Fundamentals*, 2017, available online: https://www.ashrae.org/technical-resources/ashrae-handbook/description-2017-ashrae-handbook-fundamentals.
[17] Duffie, J., Beckman, W., *Solar engineering of thermal processes*, 4th Edition, Wiley Interscience, New York, 2013.